

# Balancing Wildfire Risk and Power Outages through Optimized Power Shut-Offs

Noah Rhodes, Lewis Ntaimo and Line Roald\*

**Abstract**—Electric grid faults can be the source of catastrophic wildfires, particularly in regions with high winds and low humidity. In short-term operations, electric utilities are left with few actions to mitigate the risk of wildfires, leading to use of disruptive measures such as proactive de-energization of equipment, frequently referred to as public safety power shut-offs. Decisions of how to operate the grid in situations with high wildfire risk has significant impacts on customers, who may lose access to electricity in an attempt to protect them from the outbreak of fires. This work proposes the optimal power shut-off problem, an optimization model to support operational decision making in the context of extreme wildfire risk. Specifically, the model optimizes the operation of the grid to maximize the amount of power that can be delivered, while minimizing the risk of ignition events by selectively de-energizing components in the grid. The effectiveness of the method is demonstrated on an augmented version of the IEEE-RTS GMLC test case, located in Southern California, and compared against two simpler approaches. We observe that the optimization-based model reduces both wildfire risk and lost load shed relative to the benchmarks.

## I. INTRODUCTION

A number of tragic wildfires in recent years have highlighted the loss of life and property that may originate from electric faults. In Victoria, the 2009 Black Saturday wildfires killed 179 people. Several of those fires, including the most deadly, were sparked by electric power infrastructures [1]. In Texas, two 2011 wildfires in Bastrop county started by trees coming in contact with nearby power lines [2], and became Texas's most destructive wildfires in history, killing 4 and causing more than \$300 million in damage. In California, the 2018 Camp Fire killed 84 people, caused an estimated \$9.3 billion in residential property damage alone [3] and ultimately lead the responsible utility Pacific Gas & Electricity (PG&E) to file for bankruptcy [4] and accept charges for involuntary manslaughter [5]. This came only a year after the company's equipment started several fires in the 2017 fire season.

The risk of wildfire ignitions by power system infrastructure is exacerbated by the fact that power failures are more likely to occur during windy conditions, when wildfires spread faster and are harder to contain. As a result, research on Australian bushfires and ignition sources in California has found that fires ignited by power lines tend to be larger and more damaging than others [1], [6], [7]. Ignitions caused by power lines are not uncommon – in Texas, it is estimated that electric equipment caused more than 4,000 fires in less than 4 years [8], while PG&E identified 414 ignition events from 2015-17 [9].

Power infrastructure cause ignitions in a number of ways [10], [11], with the most common cause being contact between vegetation and conductors. Efforts to reduce probability of ignitions include improved increased inspections, more aggressive vegetation management, and changes to the protection systems to reduce the number of reclosing attempts or limit the fault current [9], [11]–[13]. However, inspections, vegetation management, and equipment upgrades must be planned over a seasonal or yearly time-scale. In a shorter time-frame, utilities are left with fewer and more disruptive actions to reduce wildfire risk. Utilities may either limit or turn off automatic reclosing entirely [9], [12], to ensure that a fault location does not experience multiple arcing events. However, this does not mitigate ignitions caused by the initial fault, nor does it avoid ignitions from high-impedance distribution line faults which may go undetected [10]. For safety during extreme conditions, the only measure that completely removes risk of fire ignitions is therefore to completely turn off a power line, as a de-energized line will not cause any sparks. After the deadly and devastating fires caused by electric power lines in 2017 and 2018, California utilities expanded the use of intentional de-energization of power lines during high-risk conditions to avoid faults that may spark new fires.

While this is arguably the only way to completely avoid the risk of ignitions, it also impacts the ability of the power system to provide reliable electricity. At their peak in October 2019, the intentional blackouts that result from de-energization, typically referred to as public power safety shut-offs (PSPS) [9], [12], turned off power to almost a million customer accounts [14]. The economic and societal impacts of a blackout on this scale, lasting for several days, is enormous, and also has important impacts on health such as increased mortality [15]. After the first major power shut-off in northern California, PG&E confirmed no less than 100 incidents of wind damage (including downed lines and contact with trees) along the 25,000 miles of power lines that were taken out of service [16]. Any of those incidents could have sparked a fire.

Given the stakes - the risk of wildfires vs the disruption of power outages - deciding which power equipment to turn off is a challenging and important task. Statements by PG&E regarding the 2019 Kincadee fire, which was likely ignited by a high-voltage transmission in an area where all distribution lines were de-energized, indicate that current operational procedures mostly consider wind speed, wildfire risk, and voltage levels when deciding which lines to turn off [17]. This raises the question of whether a more granular approach could achieve better results by considering the risk of individual components, and accounting for both the wildfire risk reduction and the load loss associated with turning a specific component off.

\*Corresponding author. Email: roald@wisc.edu

Noah Rhodes and L. Roald are with the University of Wisconsin, Madison. Lewis Ntaimo is with Texas A&M University.

This paper presents a first step towards developing this kind of more granular model, and providing a better balance between the risk of wildfires and the impact of a power outages.

Previous work on system operations under wildfire risk is surprisingly limited. Existing work has focused primarily on the impact of fires on the operation of power system equipment, such as the risk of wildfire exposure for transmission lines [18], [19], or operational impacts due to reductions in the transmission line thermal capacity as a result of heat from a nearby fire [20], [21]. While the existing work considers the challenge of operating the grid in presence of fires, this paper focuses on how power system operators can take an active role in *preventing* fires from occurring. Specifically, we provide a modeling and optimization framework to support the decision process surrounding a public safety power shut-off, with the aim of maintaining as much load delivery as possible while minimizing wildfire risk. To the best of our knowledge, this is the first paper to describe such a model.

The contributions of our paper are threefold. (1) We review existing methods for wildfire risk assessment, and extend those to estimate the relative risk associated with specific electric components. This allows us to assess the wildfire risk reduction associated with de-energizing this component. (2) We propose an optimization framework which minimizes wildfire risk, while maximizing the amount of load that can be delivered. This optimization is based on a DC power flow representation, and uses a risk parameter  $\alpha$  to weight the risk of wildfire vs the willingness to shed load. (3) We compare our method against two benchmarks on the RTS-GMLC test case, which was augmented to include data on wildfire risk. The case study demonstrates the value of accounting for both wildfire risk and impact on load shedding when determining which components to de-energize.

The remainder of the paper is organized as follows. Section II describes interactions between wildfire risk and electric grid operation, while Section III provides details on the optimization problem formulation. Section IV describes the benchmark approaches, while Sections V and VI describes the case study set-up and numerical results. Section VII summarizes and concludes, and gives an outline of future work.

## II. WILDFIRE RISK AND ELECTRIC GRIDS

The main mechanism for fire ignitions by electric power lines are electric faults, which cause sparks or arcing in a high-heat release of current. The majority of such ignitions are caused by vegetation coming into contact with power lines [9]. This leads to an unfortunate correlation between wildfire risk and electric power failures. Extreme fire conditions are characterized by low humidity and high wind conditions. Low humidity leads to a high probability that an ignition will lead to a fire, particularly in regions with fire-prone vegetation. High wind conditions imply that fires spread faster and are harder to contain. At the same time, high wind conditions cause increased movements of power lines and nearby trees, and hence increase the probability of power line faults and subsequent ignitions. This correlation between decreased ability to contain a fire and increased

probability of ignitions from power grid infrastructure is what motivates the use of proactive de-energization of equipment as a preventive, though disruptive measure. In the following, we first present our model for the wildfire risk associated with electric components, which allows us to quantify the risk reduction achieved through equipment de-energization. We then discuss the trade-off between reducing the risk and maintaining electric load delivery.

### A. Modelling Risk of Wildfire Ignitions

Our model of wildfire risk starts from a commonly used methodology for wildfire risk assessment, used e.g. by the Texas A&M Forest Service, which we extend to specifically assess the risk associated with the electric faults.

1) *Traditional Wildfire Risk Assessment*: Traditional wildfire risk models such as the Texas Wildfire Risk Assessment System (TWRAS) [22], [23] includes two components. First, the wildfire threat  $\lambda_j$  is a measure of the *likelihood* that a certain area  $j$  will burn, and depends on recent weather, as well as landscape and vegetation in the area. Second, the value response index  $\nu_j$  is associated with the *impact* of a fire on the local communities and valuable resources, and depends on both the value of resources in the considered area  $j$  (including both monetary values such as property, but also non-monetary values such as habitat of endangered species) as well as their susceptibility to sustain fire damage. Together, the likelihood  $\lambda_j$  and the impact  $\nu_j$  of the fire can be combined to determine the wildfire exposure, which we will refer to as *wildfire risk*  $\rho_j$ . For an area  $j$ , wildfire risk  $\rho_j$  is expressed as

$$\rho_j = \lambda_j \cdot \nu_j \quad (1)$$

2) *Probability of Ignitions*: While  $\lambda_j$  captures the likelihood of area  $j$  burning due to fire, it does not explicitly describe neither the *source* of ignitions, nor the associated probability. To explicitly account for specific ignition sources, we propose to express  $\lambda$  as

$$\lambda = \sum_{i \in \mathcal{I}} \pi_{i,j} \beta_j,$$

where  $\pi_{i,j}$  is the probability that an area  $j$  experiences an ignition from a specific ignition source  $i \in \mathcal{I}$ , with  $\mathcal{I}$  is the set of all possible ignition sources, and  $\beta_j$  is the probability that an ignition event causes the area  $j$  to burn. This gives rise to the following expression for the overall risk in an area  $j$ ,

$$\rho_j = \lambda_j \cdot \nu_j = \sum_{i \in \mathcal{I}} \pi_{i,j} \cdot \beta_j \cdot \nu_j \quad (2)$$

We can also express the risk associated with a single component  $e$  (potentially stretching across multiple areas) as

$$\rho_e = \sum_{j \in \mathcal{A}_e} \pi_{e,j} \beta_j \nu_j \quad (3)$$

where  $\pi_{e,j}$  represents the probability that electric component  $e$  causes an ignition in area  $j$ , the expression within the summation denotes the risk associated with component  $e$  in area  $j$ , and  $\mathcal{A}_e$  denotes the set of areas where the electric component  $e$  is present. Being able to attribute wildfire risk to specific components is important, because it allows us to use more targeted mitigation measures to reduce risk.

3) *Estimating the Risk Parameters:* For the risk assessment to be practically useful, we need to be able to estimate the parameters  $\pi_{e,j}$ ,  $\beta_j$ , and  $\nu_j$ .

To estimate the ignition probability  $\pi_{e,j}$ , we can look at historical data for ignitions, which are tracked by many utilities including PG&E [9]. For utilities which lack data on ignitions, we propose to approximate the probability of an ignition  $\pi_{e,j}$  as the probability that this component experiences a fault, which is conservative as not all faults cause ignitions [24].

To assess the wildfire risk parameters  $\beta_j$  and  $\nu_j$ , we utilize standard wildfire risk data. Organizations that manage firefighting resources calculate and publish standard metrics such as  $\rho_j$ ,  $\lambda_j$ , and  $\nu_j$  on a regular basis [23]. With this data, we approximate the probability that an area will burn as a result of a power system-related ignition to be equal to the overall likelihood that it will burn, i.e.  $\beta_j \approx \lambda_j$ . To see that this is conservative, consider the expression for  $\lambda_j = \sum_{i \in \mathcal{I}} \pi_{i,j} \beta_j$ . Isolating the term corresponding to electrical component  $e$ , we obtain

$$\pi_{e,j} \beta_j = \lambda_j - \sum_{i \in \mathcal{I}, i \neq e} \pi_{i,j} \beta_j \leq \lambda_j, \quad (4)$$

where the last inequality follows from the two probabilities  $\pi_{i,j} \geq 0$ ,  $\beta_j \geq 0$ . Since  $\pi_{e,j} \leq 1$ , equation (4) implies  $\beta_j \leq \lambda_j$ . Hence, approximating  $\beta_j \approx \lambda_j$  gives us a conservative estimate of the wildfire risk  $\mathbf{R}_e$  for a component  $e$  as

$$\mathbf{R}_e = \sum_{j \in \mathcal{A}_e} \pi_{e,j} \beta_j \nu_j \approx \sum_{j \in \mathcal{A}_e} \pi_{e,j} \lambda_j \nu_j = \sum_{j \in \mathcal{A}_e} \pi_{e,j} \rho_j. \quad (5)$$

4) *Short-Term Mitigation of Wildfire Risk:* The risk expressions (5) highlight the different options for mitigating wildfire risk. For example, mitigation measures such as increased inspections or more aggressive vegetation management around power lines can help both reduce the probability of faults and subsequent ignitions, hence reducing  $\pi_{e,j}$ . From a firefighting perspective, other measures such as prescribed burns, improved early warning system or an increase in the available fire fighting resources can help reduce the probability that an ignition will lead to a widespread fire, leading to a reduction in  $\rho_j$ . However, these mitigation measures take time to plan for and implement.

In short-term operations, operators have fewer options, with the most effective (and most disruptive) being de-energization of equipment. If a component is de-energized,  $\pi_{e,j}$  is reduced to zero, as there will not be any faults. The decision on whether to keep a component energized can hence be understood as a decision related to whether or not we are willing to accept the risk  $\mathbf{R}_e$ . With this consideration, we express as

$$\mathbf{R}_e = \begin{cases} \sum_{j \in \mathcal{A}_e} \pi_{e,j} \rho_j & \text{if } e \text{ is energized} \\ 0 & \text{if } e \text{ is de-energized} \end{cases} \quad (6)$$

For generators, lines, and buses, we represent the decision of whether or not to de-energize the equipment through binary decision variables  $z_* \in \{0, 1\}$  that indicate whether a certain component is energized or not, with  $z_g$ ,  $z_l$ , and  $z_i$  denoting the variables for generators, lines, and buses, respectively. In the case of loads, we assume that the load seen by the operator is representative of a large number of individual loads. We therefore model load shedding as a continuous variable  $x_d \in$

$[0, 1]$  that represent the fraction of the load (and corresponding distribution infrastructure) that is de-energized.

This allows us to model  $R_{Fire}$ , the total wildfire risk arising from electric components, as

$$R_{Fire} = \sum_{d \in \mathcal{D}} x_d \mathbf{R}_d + \sum_{g \in \mathcal{G}} z_g \mathbf{R}_g + \sum_{l \in \mathcal{L}} z_l \mathbf{R}_l + \sum_{i \in \mathcal{B}} z_i \mathbf{R}_i. \quad (7)$$

where  $\mathcal{D}$ ,  $\mathcal{G}$ ,  $\mathcal{L}$ , and  $\mathcal{B}$  represent the sets of load demand, generators, transmission lines, and buses, respectively.

### B. Modelling Risk of Power Shut-Offs

De-energizing loads and electric equipment not only reduces wildfire risk, but also limits the ability of the system to provide electricity to customers, leading to power shut-offs. It is very hard to obtain detailed and accurate estimates of the economic and societal impact of such power shut-offs. The cost depends on a number of factors, including the frequency and duration of such shut-offs, as well as the value the electricity provides to individual customers. Here, we refrain from a detailed monetary assessment of the economic impact of lost load, and aim to deliver as much load as possible. Our variable  $D_{Tot}$  represents the total amount of load delivered, and is expressed by

$$D_{Tot} = \sum_{d \in \mathcal{D}} x_d w_d \mathbf{D}_d, \quad (8)$$

where  $\mathbf{D}_d$  is the amount of load served under normal operating conditions. We include the weight  $w_d$  to express that certain loads, such as hospitals or other essential services, may be prioritized over others.

### C. Trading off Risk of Wildfires and Power Shut-Offs

With the above considerations, we can express the trade-off between maximizing load delivery and minimizing wildfire risk as

$$\max(1 - \alpha) D_{Tot} - \alpha R_{Fire} \quad (9)$$

Here, the parameter  $\alpha \in [0, 1]$  expresses the trade-off between serving more load (low  $\alpha$ ) and avoiding wildfire risk (high  $\alpha$ ).

We note that although the approximations of the wildfire risk associated with each component may seem crude and potentially very conservative, the absolute risk values in the above model are less important than the relative differences in risk among different electric grid components. Furthermore, by solving the model for different values of  $\alpha$ , we obtain a Pareto front of solutions that represent optimal trade-offs between continued load delivery and reductions in wildfire risk.

## III. OPTIMAL POWER SHUT-OFFS

Based on the above modelling, we now present the optimal power shut-off problem, an optimization framework to aid decisions related to public power safety shut-offs. We approach the optimization problem from the perspective of a power system operator, whose main objective is to maximize load delivery while minimizing wildfire risk as expressed by (9). The time frame of this decision is making short-term operations, ranging from a few days ahead of real-time until

intraday operation. The decision variables are  $z_g, z_l, z_i$  and  $x_d$ , representing whether or not individual components will remain energized or not, as well as the power generation of the generators  $P_g^G$ ,  $g \in \mathcal{G}$ , the power flows on transmission lines  $l \in \mathcal{L}$  from bus  $j$  to bus  $i$  given by  $P_{l,i,j}^L$  and the voltage angles  $\theta_i$ ,  $i \in \mathcal{B}$ . In the following, we present the constraints of our model, and summarize the full optimization problem.

1) *Component interactions*: Generators, loads and lines can only be energized if the buses they are connected to are energized. We enforce this through the following constraints,

$$z_i \geq x_d \quad \forall d \in \mathcal{B}_i^D, \quad \forall i \in \mathcal{B} \quad (10a)$$

$$z_i \geq z_g \quad \forall g \in \mathcal{B}_i^G, \quad \forall i \in \mathcal{B} \quad (10b)$$

$$z_i \geq z_l \quad \forall l \in \mathcal{B}_i^L, \quad \forall i \in \mathcal{B} \quad (10c)$$

The sets  $\mathcal{B}_i^D$ ,  $\mathcal{B}_i^G$ , and  $\mathcal{B}_i^L$  represent the set of loads, generators, and lines connected to bus  $i$ , respectively.

2) *Generators*: The generator limits are given by

$$z_g \underline{P}_g \leq P_g^G \leq z_g \overline{P}_g \quad \forall g \in \mathcal{G} \quad (11)$$

which enforces that  $P_g = 0$  if the generator is turned off, and otherwise enforces the maximum and minimum generation limits denoted by  $\overline{P}_g, \underline{P}_g$ .

3) *Power flow representation and transmission limits*: To represent the power flow in the system, we utilize a DC power flow representation, extended to model the on/off status of loads, generators, lines or buses. This gives rise to the following set of equations,

$$P_{l,i,j}^L \leq -b_l(\theta_i - \theta_j + \theta^{Max}(1 - z_l)) \quad \forall l \in \mathcal{B}_{i,j}^L \quad (12a)$$

$$P_{l,i,j}^L \geq -b_l(\theta_i - \theta_j + \theta^{Min}(1 - z_l)) \quad \forall l \in \mathcal{B}_{i,j}^L \quad (12b)$$

$$-T_l z_l \leq P_{l,i,j}^L \leq T_l z_l \quad \forall l \in \mathcal{L} \quad (12c)$$

$$\sum_{g \in \mathcal{B}_i^G} P_g^G + \sum_{l \in \mathcal{B}_i^L} P_{l,i,j}^L - \sum_{d \in \mathcal{B}_i^D} x_d D_d = 0 \quad \forall i \in \mathcal{B} \quad (12d)$$

Eqs. (12a)-(12c) represent the power flow  $P_{l,i,j}$  on line  $l$  from bus  $i$  to bus  $j$ , with  $b_l$  representing the susceptance of the line. We note that if line  $l$  is energized, i.e.  $z_l = 1$ , (12a) and (12b) correspond to the standard DC power flow constraint, and the power flow is limited to be within the thermal power flow limit  $T_l$  by (12c). If the line is de-energized,  $z_l = 0$ , we relax (12a), (12b) by adding constants  $\theta^{Max}, \theta^{Min}$  to the angle differences, such that these constraints can never be binding. Further, for  $z_l = 0$ , (12c) the power flow  $P_{l,i,j}$  is set to zero. The nodal power balance is represented in equation (12d), where the variable  $x_d$  represents the fraction of the load  $D_d$  that is shed.

4) *Optimal Power Shut-Off Problem*: With the above modeling considerations, the full optimization problem is given by

$$\begin{aligned} \max_{x, z, P^G, P^L, \theta} \quad & (1 - \alpha) D_{Tot} - \alpha R_{Fire} \quad (9) \\ \text{s.t.:} \quad & \text{Component relationship: (10)} \quad (\text{OPS}) \\ & \text{Generator constraints: (11)} \\ & \text{Power flow constraints: (12)} \end{aligned}$$

We note that this is a mixed-integer linear program (MILP), with integer variables for all components in the system.

## IV. BENCHMARK METHODS

We compare the optimal power shut-off (13) problem against two heuristics. An important difference between these heuristics and the OPS model is that neither of these heuristics considers the impact on the ability of the system to serve the load. The decisions on which components are turned on or off are taken solely based on wildfire risk, without consideration of how much load will be shed as a result.

1) *Area Heuristic (AH)* The first benchmark is a very basic heuristic that computes the overall wildfire risk of an entire area of the electric grid, and shuts down all components within that area if the risk is above a pre-defined threshold.

2) *Transmission Heuristic (TH)* The second benchmark is slightly more sophisticated, and is inspired by accounts of the public safety power shut-offs in the area around the Kincade fire [17]. In this benchmark, all transmission lines are compared against a risk threshold that varies by voltage level, where lines operated at lower voltages have a lower risk threshold due to narrower right of ways and closer proximity to vegetation. If a line exceeds the pre-fixed risk thresholds, it is deactivated. In this model, we do not directly shut down loads, generators or buses, except when they have to be shut down due to lack of interconnection.

To solve these benchmark problems, we first evaluate the wildfire risk associated with each region/transmission line according to (5), and compare it against the risk thresholds to determine which components will be turned off. We then solve the maximum load delivery (MLD) problem from [25], which maximizes load delivery for the remaining system. In this problem, additional loads, generators, buses or lines may be turned off if they lack interconnection. Based on the solution, we evaluate the total delivered load (8) and the remaining wildfire risk (7).

## V. CASE STUDY: IMPLEMENTATION AND SETUP

### A. Implementation

The Optimal Power-Shutoff Problem and the accompanying heuristics are implemented the Julia programming language [26] using JuMP [27], and is part of a new package PowerSystemWildfireRisk.jl which we plan to release in conjunction with this paper. This package also relies heavily on the PowerModels.jl packages [28]. The network plots are generated using a modified version of PowerModelsAnalytics.jl. The maximum load delivery problem [25] is solved using PowerModelsRestoration.jl.

Both the optimal power shut-off (13) problem and the maximum load delivery (MLD) problem used for the heuristics are a mixed-integer linear programs. These problems were all solved in Julia v1.2 using the Gurobi v8.1 optimizer [29] on a machine with a 12-thread Intel CPU @3.2 GHz and 16 GB of memory. With this setup, the optimization-based power shut-off problem solves in  $< 0.5s$ , while maximum load delivery problem solves in  $< 0.05s$ .

### B. System model with wildfire risk

To create a case study of system with high wildfire risk, we start with the RTS-GMLC 96-bus case [30]. For our base case

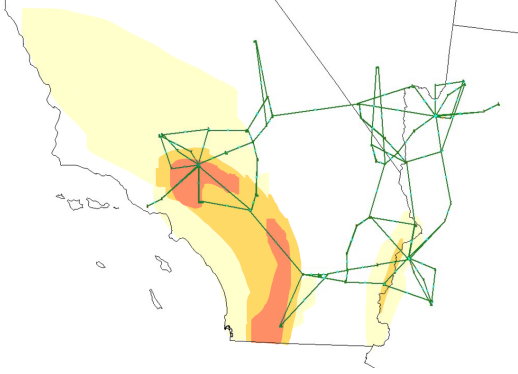


Fig. 1: **Wildfire Risk Map** Power grid test case plotted over a representative wildfire risk map for Southern California, based loosely on data in [32].

grid, we utilize the standard system configuration as given in the MatPower case file, but omit the HVDC line. The values for  $\theta^{Max}$  and  $\theta^{Min}$  are the maximum possible angle differences that could appear between any two nodes in the system, calculated as described in [31].

The RTS-GMLC system is provided with geographic coordinates and is located in southern California, Nevada, and western Arizona as shown on the map in Fig. 1. To associate this test case with realistic values for wildfire risk, we created an artificial wildfire risk map, inspired by a map for Southern California from October 2019 [32]. This map is drawn underneath the power lines in Fig. 1. The wildfire risk levels include low risk (white), medium risk (yellow), high risk (orange), and extreme risk (dark orange). The western region of the map has a very high risk, while there is also a region with moderate wildfire risk at the border to Arizona.

We consider the low risk regions to be business-as-usual with wildfire risk  $\rho_j = 0.0$ , and assign wildfire risk values  $\rho_j$  of 1.0, 2.0 and 4.0 for the medium, high, and extreme risk zones. These risk values are then associated with the power system components and their assumed fault probabilities to present the risk of these devices igniting a wildfire.

We assume for simplicity that all generators and buses (i.e., substations) have the same probability  $\pi_{e,j}$  of starting an ignition. Since we are mostly concerned about the relative risk between different components, we assume for simplicity that  $\pi_{e,j} = 1$ . For the buses and generators, the wildfire risk coefficient is determined by their locations on the risk map, e.g. bus  $i$  in the extreme risk zone  $j$  with wildfire risk  $\rho_j = 4.0$  has a component risk given by  $R_i = \pi_{e,j}\rho_j = 4.0$ . For the loads, we may consider assigning a higher probability of ignition to a larger load (as a large load is indicative of a larger distribution system). However, other factors than the load size, such as whether a load represents an urban distribution grid with mostly underground cables or a rural community with long high-risk lines, also play a major role in the ignition probability and is not given as part of the available data. For simplicity, we therefore assume  $\pi_{d,j} = 1$  (i.e., the ignition probability is assumed to be similar to the generators and buses). As an example, a load in a high risk area with  $\rho_j = 2.0$  has a component risk of  $R_d = \pi_{d,j}\rho_j = 2.0$ . Further, we set

the weights  $w_d = 1$  for all loads.

For transmission lines, we assume that the probability of ignition is influenced both by the voltage level and the length of the lines. We assume that the probability of ignition  $\pi_{l,j}$  is uniform along the lines, and that each 10km segment of the line counts as an area  $j$  with corresponding wildfire risk  $\rho_j$ . We choose  $\pi_{l,j} = 1.0$  for the 230 kV lines and  $\pi_{l,j} = 2.0$  for the 138 kV lines, indicating that the lower voltage lines have a higher probability of ignitions relative to the high voltage lines. We then calculate the component risk  $R_l$  using (5).

## VI. CASE STUDY: NUMERICAL RESULTS

Using the test case presented above, we now assess the benefit of optimizing the public safety power shut-off under consideration of both wildfire risk and resulting load shedding. To do this, we solve the case study problem using both the optimized power shut-off (OPS) method, the area heuristic (AH) and the transmission heuristic (TH).

For the optimal power shut-off, we need to choose  $\alpha$ , which determines the trade-off between wildfire risk and load delivery. To determine good choices of the  $\alpha$  parameter, we solve problem (13) with values of alpha ranging from 0 to 1 in steps of 0.01 to obtain a Pareto curve, which describes the optimal trade-off between wildfire risk and load delivery. For the transmission heuristic, we need to select a threshold risk value  $R_l^{max}$  beyond which we choose to shut off the line. To determine good choices of  $R_l^{max}$ , we solve the problem with values for  $R_l^{max}$  ranging between 100 and 1 in steps of 1. For the area heuristic, we select a risk threshold that disable devices in the high-risk region (corresponding to area 3 in the RTS-GMLC network). We also compare our results with just maintaining standard operation, where all components are operational and all load is served.

### A. Pareto Front

To compare the results, we first look at the trade-off between load delivery and wildfire risk obtained with the optimal power shut-off, the transmission heuristic and the area heuristic. Fig. 2 (a) shows the Pareto front obtained for the optimal power shut-off with varying values of  $\alpha$  (blue), the transmission heuristic with varying risk thresholds  $R_l^{max}$  (orange), as well as the operating point of the area heuristic, which is only a single point (green). From the Pareto front, we observe that a significant reduction in risk can be achieved with no, or very little, load shedding, both with the optimal power shut-off and the transmission heuristic. However, the optimal power shut-off method consistently achieves a lower risk level for the same amount of load delivery. The area heuristic performs much poorer than the other two methods, resulting in both higher load shed and higher wildfire risk.

### B. Operation Schemes

In Fig. 2 (a), five points are selected for further analysis and are indicated by a star. The selected solutions correspond to a medium and a low risk scenario for the optimal power shut-off and the transmission heuristic, as well as the solution

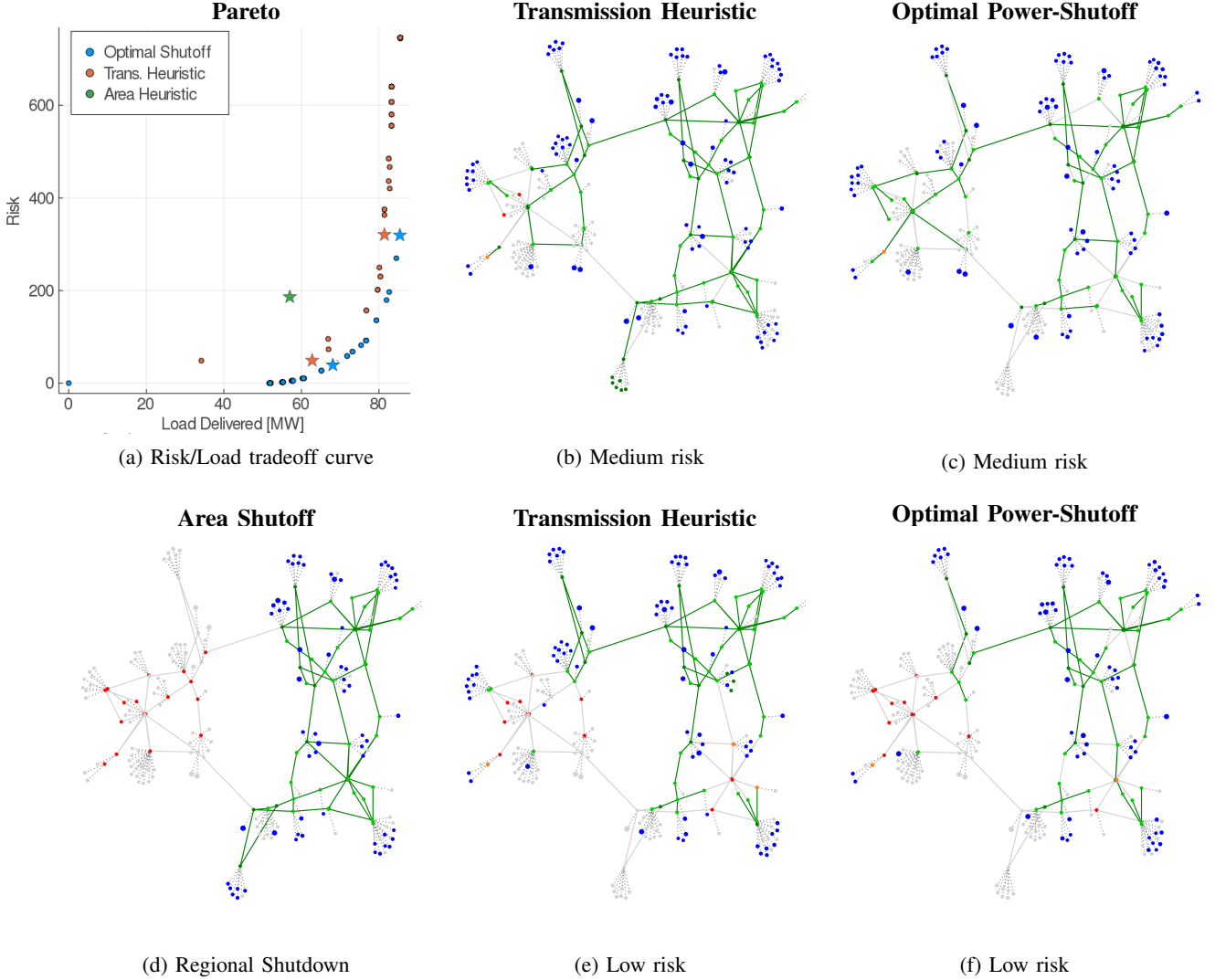


Fig. 2: Plot (a): Trade-off between load delivery and wildfire risk, as obtained with the optimal power shut-off problem with different values of  $\alpha$  (blue), the transmission heuristic with different values of  $R_l^{max}$  (orange) and area heuristic (green). The stars denote the solutions for which we plot the resulting topology. Plots (b)-(f): System topology for the medium-risk solutions (top) and low-risk solutions (bottom), with area heuristic (left), transmission heuristic (middle) and optimal power shut-off (right). Inactive components are shown in gray, while active items are shown in green (transmission lines) and blue (generators). Green, orange and red color for the buses indicate delivery of all, some or no load.

to the area heuristic. For these scenarios, we plot the resulting network topologies, which are shown in Fig. 2 (b)-(f). Here, inactive components are shown in gray, while active items are shown in green. Buses with a light-green color fully satisfy load, those in orange have partial load shed, while those in red represent when load is completely shed. The blue nodes represent active generators, and the attached bus is indicated with a dashed line. Table I lists the total risk, load served, and solve time for those grid scenarios.

1) *Medium-Risk Operation Schemes*: We first compare the two medium risk scenarios obtained with the optimal power shut-off and the transmission heuristic. As we observe from Table I, these two scenarios have a similar wildfire risk level, but the optimal power shut-off serves more load than the transmission heuristic. Both cases reduce wildfire risk by 50% relative to standard operation (where all components are energized), at the expense of a reduction in the delivered load

from 85.5 MW in standard operation to 85.4 MW for the optimal power shut-off (0.1 MW load shed) and 81.4 MW for the transmission heuristic (4.1 MW load shed). We see that the optimal power shut-off serve almost the entire load, while reducing the risk by half.

To better understand the differences between the two solutions, we examine the topologies of the energized grid, which are seen in Fig. 2 (b) and (c). These figures reveal significant differences in how load is served. The transmission heuristic in Fig. 2 (b) primarily disables lines in the high-risk western region, and isolates some loads, shown in red. The network in the other regions is almost untouched. In comparison, the optimal power shut-off in Fig. 2 (c) has only 0.1 MW of load shed, and reduces the network to a near-radial, tree-like structure. To serve the load at minimal risk, more components in lower risk zones are disabled, but this is done in a way which allows for almost full load delivery. One important thing

TABLE I: Total risk and load served for selected operating points

	Total Risk	Load Served	Solve Time
Standard Operation	746.2	85.5 MW	N/A
<b>Medium wildfire risk</b>			
Optimal Power Shutoff	319.5	85.4 MW	0.36 sec
Transmission Heuristic	320.6	81.4 MW	0.04 sec
<b>Low wildfire risk</b>			
Optimal Power Shutoff	38.9	68.1 MW	0.27 sec
Transmission Heuristic	48.8	62.3 MW	0.03 sec
Area Heuristic	186.1	57.0 MW	0.04 sec

to note is that the optimal power shut-off removes redundancy in the system in order to reduce risk, and is therefore no longer N-1 secure. While losing this redundancy negatively impacts system reliability, it is preferable to an intentional blackout.

2) *Low-Risk Operation Schemes:* We next examine the two low-risk solutions obtained with the optimal power shut-off solutions and the transmission heuristic, respectively. These low-risk solutions were chosen to have a similar risk level, as can be seen in Table I. We first observe that relative to the medium risk case, the wildfire risk is reduced by almost an order of magnitude, but at the expense of delivering much less load. The transmission heuristic delivers only 62.3 MW load (corresponding to 23.2 MW load shed), while the optimal power shut-off achieves 68.1 MW load delivery (corresponding to 17.3 MW load shed). We conclude that the optimal power shut-off reduces load shed by 25% relative to the transmission heuristic at comparable risk levels.

When examining the system topologies of the low-risk solutions in Fig. 2 (e) and (f), we observe that both methods shut down almost all components in the high-risk western region. Both approaches also choose to island some regions of the grid, based on the ability of nearby generation to support the load. The main difference between the two solutions is that the optimized strategy is able to prioritize shut-off of components that have a lower impact on load delivery.

We note that the assumption that the grid can operate in multiple islands may or may not be realistic, depending on the generators ability to maintain stable operation, and procedures for resynchronization once the wildfire risk is less acute. However, this result highlights how geographically distributed generation can support local load during large-scale disruptions to the grid.

3) *The value of a granular approach:* We next take a closer look at the three grid topologies shown in the bottom part of Fig. 2, which from left to right represent an increasingly granular approach to public safety power shutdown. The area heuristic in Fig. 2 (d) shuts down an entire region based on a simple threshold, while the transmission heuristic in Fig. 2 (e) considers the risk values of individual lines. The optimal power shut-off in Fig. 2 (f) considers both the risk of individual components as well as their impact on the system's ability to serve the load. Comparing the grid topologies and the values shown in Table I, we observe that including mode detail consistently reduces risk *and* increases load delivery.

TABLE II: Total wildfire risk for different types of devices in the solutions obtained with the optimal power shut-off problem.

Optimal Power Shut-Off	Total	Bus	Line	Gen.	Load
Medium Wildfire Risk	319.5	52.0	181.7	26.0	59.9
Low Wildfire Risk	38.9	11.0	8.1	8.0	11.8

### C. Optimal Power Shut-Off Solutions

To better understand the optimal power shut-off solutions, we investigate how the total risk is distributed among the different component types. Table II shows the risk is associated with each component type in the medium and low risk solutions. The two cases differ mainly in how much wildfire risk is associated with transmission lines. Transmission lines contribute 57% of the total risk in the medium-risk case, compared with only 20% in the low-risk case.

To understand transmission line risk in more detail, we plot the risk coefficient  $R_l$  for each line against the amount of power carried by this line,  $P_{l,i,j}^L$ . The result is shown in Fig. 3, with the medium risk solution on the left and the low risk solution on the right. The energized transmission lines are represented by blue dots and de-energized lines are plotted in orange (note that  $P_{l,i,j}^L = 0$  for de-energized lines). From these plots, we first observe that the risk values of the lines vary between 0 and 53, with most lines concentrated at lower values. We notice that the low-risk solution turns off essentially all high-risk power lines, while the medium risk solution allows even some of the highest risk lines continue to operate. Further, we see that the threshold for when the lines are turned off is not given by the absolute risk value of the line (as it is in the threshold heuristic), but is rather a function of both the risk value of the line and the amount of power transferred by the line. In particular, higher risk lines are allowed to operate only if they transfer a significant amount of power, and thus contribute significantly to increase the amount of delivered load, while low risk lines also operate at lower power transfer levels.

## VII. CONCLUSIONS AND FUTURE WORK

This work uses optimization to minimize wildfire risk due to electric power system components, while maintaining electricity supply to as many customers as possible. Specifically, we propose to utilize extensions of existing models for wildfire risk to assign risk values to individual electrical components, which allows us to assess the reduction in wildfire risk that is achieved by de-energizing the component. Utilizing these risk values, we formulate the optimal power shut-off problem, which is similar to an optimal power flow with additional decision variables to represent whether or not a component is energized. The objective is to minimize wildfire risk, while maximizing load delivery. This proposed approach is demonstrated on the RTS-GMLC test case, which is combined with data from a wildfire risk map. The optimal power shut-off problem is compared against two heuristic decision models which disable specific components based on their wildfire risk value alone. The results show that the optimal power shut-off problem, which considers both the wildfire risk value and the impact of the component on the delivered load, is able to



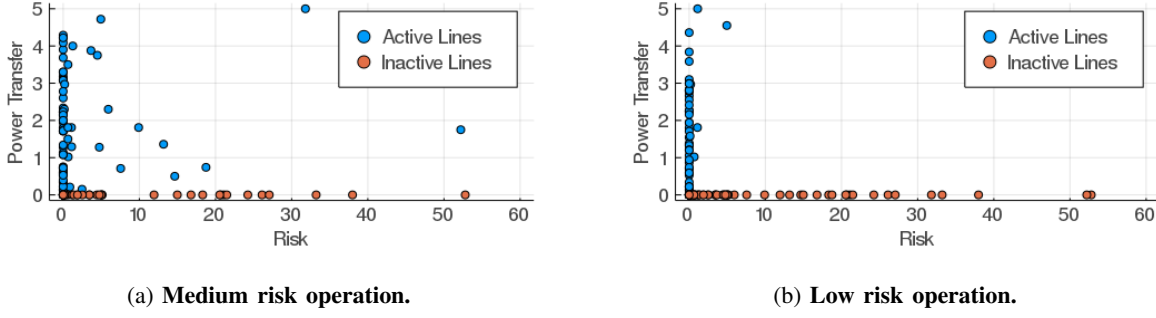


Fig. 3: Scatter plot showing the wildfire risk (horizontal axis) and the power transferred (vertical axis) for each transmission line.

serve more load at lower risk values. We also observe that the network topology which serves load at minimal risk has a tree-like structure, and sometimes splits the system into islands.

We consider our model as a first, important step to better understand how power system operations can be modified to minimize wildfire risk, at minimal disruption to customers. However, the paper also opens a number of important avenues for future work. We believe that it is important to better understand how the probability of wildfire ignitions from power system equipment change based on external conditions, such as local weather conditions and landscape characteristics, and conditions we can control, such as vegetation management, maintenance schedule or settings for post-fault automatic reclosing. This would enable a more detailed calculation of the component wildfire risk, and extensions of our optimization framework to include additional operational decisions, such as whether or not to disable automatic reclosing. Further, we would also like to include considerations such as N-1 security (which are particularly likely to occur if the fault probability is high) or extensions required to consider wildfire risk in distribution grids.

## REFERENCES

- [1] B. G. Teague, R. N. McLeod, and S. M. Pascoe, *Final Report: 2009 Victorian Bushfires Royal Commission*. Victorian Bushfires Royal Commission, Australia, 2010. [Online]. Available: <https://bit.ly/2JWEjON>
- [2] CBC. (2011) Texas wildfire likely caused by power line sparks. [Online]. Available: <https://www.cbc.ca/news/world/texas-wildfire-likely-caused-by-power-line-sparks-1.998388>
- [3] T. Jeffery, S. Yerkes, D. Moore, F. Calgiano, and R. Turakhia, "2019 Wildfire Risk Report," Tech. Rep., 2019. [Online]. Available: <https://www.corelogic.com/insights-download/wildfire-risk-report.aspx>
- [4] Pacific Gas and Electric Company. (2019) Press release: PG&E Files for Reorganization Under Chapter 11. [Online]. Available: <https://bit.ly/2JSizDy>
- [5] —. (2020) Press release: PG&E Reaches Plea Agreement on State Charges Related to 2018 Camp Fire. [Online]. Available: <https://bit.ly/2URsEqJ>
- [6] C. Miller *et al.*, "Electrically caused wildfires in Victoria, Australia are over-represented when fire danger is elevated," *Landscape and Urban Planning*, vol. 167, pp. 267–274, 2017.
- [7] J. E. Keeley and A. D. Syphard, "Historical patterns of wildfire ignition sources in California ecosystems," *Int. J. of Wildland Fire*, vol. 27, no. 12, pp. 781–799, 2018.
- [8] Texas Wildfire Mitigation Project. (2014) How do power lines cause wildfires? [Online]. Available: <https://bit.ly/3b1KT7b>
- [9] Pacific Gas and Electric Company, "Pacific Gas and Electric Company Amended 2019 Wildfire Safety Plan," Tech. Rep., 2019.
- [10] B. D. Russell, C. L. Benner, and J. A. Wischkaemper, "Distribution feeder caused wildfires: Mechanisms and prevention," in *65th Annual Conference for Protective Relay Engineers*, 2012, pp. 43–51.
- [11] S. Jazebi, F. de Len, and A. Nelson, "Review of Wildfire Management Techniques Part I: Causes, Prevention, Detection, Suppression, and Data Analytics," *IEEE Trans. Power Delivery*, vol. 35, no. 1, pp. 430–439, 2020.
- [12] Southern California Edison Company, "Southern California Edison Company's 2019 Wildfire Mitigation Plan," Tech. Rep., 2019.
- [13] Pacific Gas and Electric Company, "Pacific Gas and Electric Company 2020 Wildfire Mitigation Plan Report," Tech. Rep., 2020.
- [14] California Public Utilities Commission. (2020) Deenergization (PSPS). [Online]. Available: <https://www.cpuc.ca.gov/deenergization/>
- [15] G. B. Anderson and M. L. Bell, "Lights out: impact of the August 2003 power outage on mortality in New York, NY," *Epidemiology*, vol. 23, no. 2, pp. 189–193, 2012.
- [16] B. Johnson. (2019) We hear the anger, are working hard to avoid power shut-offs. [Online]. Available: <https://bit.ly/2UZDla>
- [17] San Francisco Chronicle. (2019) Pg&e transmission tower broke near origin of kincade fire. [Online]. Available: <https://bit.ly/2Xvac8X>
- [18] J. A. Sathaye *et al.*, "Rising temps, tides, and wildfires: Assessing the risk to California's energy infrastructure from projected climate change," *IEEE Power and Energy Magazine*, vol. 11, no. 3, pp. 32–45, 2013.
- [19] S. Dian *et al.*, "Integrating wildfires propagation prediction into early warning of electrical transmission line outages," *IEEE Access*, vol. 7, pp. 27 586–27 603, 2019.
- [20] M. Choobineh and S. Mohagheghi, "Power grid vulnerability assessment against wildfires using probabilistic progression estimation model," in *IEEE PES General Meeting*, 2016.
- [21] D. N. Trakas and N. D. Hatziaargyriou, "Optimal distribution system operation for enhancing resilience against wildfires," *IEEE Trans. on Power Systems*, vol. 33, no. 2, pp. 2260–2271, 2017.
- [22] J. A. G. Arrubla, L. Ntamo, and C. Stripling, "Wildfire initial response planning using probabilistically constrained stochastic integer programming," *Int. J. of Wildland Fire*, vol. 23, no. 6, pp. 825–838, 2014.
- [23] Texas A&M Forest Service. Texas wildfire risk assessment portal. [Online]. Available: <https://www.texaswildfirerisk.com/>
- [24] D. Coldham, A. Czerwinski, and T. Marxsen, "Probability of bushfire ignition from electric arc faults," HRL Technology Pty Ltd, Tech. Rep., 2011. [Online]. Available: <https://bit.ly/2xel5kY>
- [25] C. Coffrin, R. Bent, B. Tasseff, K. Sundar, and S. Backhaus, "Relaxations of ac maximal load delivery for severe contingency analysis," *IEEE Trans. on Power Systems*, vol. 34, no. 2, pp. 1450–1458, 2019.
- [26] J. Bezanson, A. Edelman, S. Karpinski, and V. Shah, "Julia: A fresh approach to numerical computing," *SIAM Review*, vol. 59, no. 1, pp. 65–98, 2017. [Online]. Available: <https://doi.org/10.1137/141000671>
- [27] I. Dunning, J. Huchette, and M. Lubin, "Jump: A modeling language for mathematical optimization," *SIAM Review*, vol. 59, no. 2, pp. 295–320, 2017.
- [28] C. Coffrin, R. Bent, K. Sundar, Y. Ng, and M. Lubin, "Powermodels.jl: An open-source framework for exploring power flow formulations," in *Power Systems Computation Conference (PSCC)*, June 2018.
- [29] Gurobi Optimization, Inc., "Gurobi optimizer reference manual," Published online at <http://www.gurobi.com>, 2014.
- [30] C. Barrows *et al.*, "The IEEE reliability test system: A proposed 2019 update," *IEEE Trans. Power Systems*, vol. 35, no. 1, pp. 119–127, 2020.
- [31] H. Hijazi, C. Coffrin, and P. Van Hentenryck, "Convex quadratic relaxations for mixed-integer nonlinear programs in power systems," *Math. Prog. Computation*, vol. 9, no. 3, pp. 321–367, 2017.
- [32] P. Duginski, "Extremely critical fire weather will continue Thursday in Southern California," *Los Angeles Times*, Oct 2019. [Online]. Available: <https://lat.ms/2V0jYhJ>